



Damage Prediction Using Several Types of Macro-scale Damage Models in Different Cold Wire Production Lines

Trong-Son Cao, Pierre Montmitonnet, Pierre-Olivier Bouchard, Christian Bobadilla, Christophe Vachey

► To cite this version:

Trong-Son Cao, Pierre Montmitonnet, Pierre-Olivier Bouchard, Christian Bobadilla, Christophe Vachey. Damage Prediction Using Several Types of Macro-scale Damage Models in Different Cold Wire Production Lines. 11th International Conference on Technology of Plasticity, ICTP 2014, Oct 2014, Nagoya, Japan. pp.185-190, 10.1016/j.proeng.2014.09.148 . hal-01110924

HAL Id: hal-01110924

<https://minesparis-psl.hal.science/hal-01110924>

Submitted on 27 Oct 2015

HAL is a multi-disciplinary open access archive for the deposit and dissemination of scientific research documents, whether they are published or not. The documents may come from teaching and research institutions in France or abroad, or from public or private research centers.

L'archive ouverte pluridisciplinaire **HAL**, est destinée au dépôt et à la diffusion de documents scientifiques de niveau recherche, publiés ou non, émanant des établissements d'enseignement et de recherche français ou étrangers, des laboratoires publics ou privés.

11th International Conference on Technology of Plasticity, ICTP 2014, 19-24 October 2014,
Nagoya Congress Center, Nagoya, Japan

Damage prediction using several types of macro-scale damage models in different cold wire production lines

Trong-Son Cao^a, Pierre Montmitonnet^{a*}, Pierre-Olivier Bouchard^a, Christian Bobadilla^b,
Christophe Vachey^c

^a CEMEF, MINES ParisTech, UMR CNRS 7635, CS 10207, 06904 Sophia-Antipolis Cedex, France

^b ArcelorMittal Long Carbon R&D, Rue des Serruriers, 57175 Gandrange, France

^c UGITECH Research Centre, avenue Paul Girod, 73403 Ugine Cedex, France

Abstract

The purpose of the present paper is to show how and to what extent the introduction of refined, shear sensitive models improves on previous ones, based on triaxiality only, for the phenomenological description of ductile damage in bulk cold metal forming processes. Wire-drawing and wire rolling are taken as examples. A set of mechanical tests has been conducted: round bar tension, notched bar tension, plane strain tension, and torsion for pure shear deformation. Both constitutive and damage model parameters have been carefully identified, with back-computation of the laboratory tests for validation. Application of the models to the cold forming processes, described here, shows the superiority of the shear-enhanced models for locating maximum damage in flat wire rolling, where a significant amount of shear is present ("blacksmith's cross" deformation pattern). On the contrary, it proves unnecessary for low-shear processes such as wire-drawing. The cavity-growth Gurson-Tvergaard-Needleman model seems to be the best basis for damage prediction in patented high carbon steel, a very ductile material.

© 2014 The Authors. Published by Elsevier Ltd. This is an open access article under the CC BY-NC-ND license (<http://creativecommons.org/licenses/by-nc-nd/3.0/>).

Selection and peer-review under responsibility of the Department of Materials Science and Engineering, Nagoya University

Keywords: Ductility; Damage; Triaxiality; Lode angle; Wire-drawing; Wire rolling; Pearlite steel; Stainless steel.

* Corresponding author. Tel. : +33-4-93-95-7414 ; fax : +33-4-92-38-9752
E-mail address : pierre.montmitonnet@mines-paristech.fr

1. Survey of mechanical damage models

Ductile fracture is often met in cold forming. It is due mainly to cavity nucleation and growth from inclusions. Its quantitative prediction in complex strain and stress fields as found in bulk metal forming processes remains a difficult task. Once identified under certain conditions, a damage model is often found to fail in slightly different situations. The reason is that most phenomenological models are over-simplified, accounting for only a very crude summary of the state of stress and strain, such as triaxiality-based models (Lemaitre (1986)). Recently, emphasis has been put on models including all stress invariants, e.g. with triaxiality and Lode angle, see Bai and Wierzbicki (2008) or Xue (2007). Another way of dealing with the cavitation – growth – coalescence sequence is the Gurson compressible plasticity model as in Needleman and Tvergaard (1984); it has also been enriched in a phenomenological way recently, to become more sensitive to the specific effects of shear (Nahshon and Hutchinson (2008), Xue (2008)). The purpose of the present paper is to examine the capacity of these different types of models to predict damage and fracture in two different processes, wire-drawing and wire rolling.

2. Damage models compared

Six ductile damage models are compared in the following. They are described in terms of invariants of the stress tensor σ , such as $\left(\frac{-p}{\bar{\sigma}}, \bar{\sigma}, \bar{\theta}\right)$: triaxiality, equivalent (von Mises) stress ($\bar{\sigma}$), Lode parameter ($\bar{\theta}$). p is the hydrostatic pressure. With $\sigma_1 \geq \sigma_2 \geq \sigma_3$ the three principal stresses of σ , the Lode parameter is defined by:

$$\bar{\theta} = -\frac{6}{\pi} \cdot \tan^{-1} \left(\frac{1}{\sqrt{3}} \frac{2\sigma_2 - \sigma_1 - \sigma_3}{\sigma_1 - \sigma_3} \right), \quad (1)$$

2.1. Lemaitre and enhanced Lemaitre model

In the enhanced Lemaitre model (LEL model) where the Lode parameter is taken into account (Cao et al. (2014a)), a modified damage potential F_D is defined, from which the damage rate is deduced according to the normality rule:

$$F_D = \frac{s}{(s+1)(1-D)} \cdot \frac{\left(\frac{Y}{S}\right)^{s+1}}{\alpha_1 + \alpha_2 \bar{\theta}^2}, \quad Y = \frac{\bar{\sigma}^2}{2E \cdot (1-D)^2} \cdot \left[\frac{2}{3} \cdot (1 + \nu) + 3(1 - 2\nu) \cdot \left(\frac{-p}{\bar{\sigma}}\right)^2 \right], \quad (2a,b)$$

$$\dot{D} = \dot{\lambda} \frac{\partial F_D}{\partial Y} = \frac{\dot{\lambda}}{1-D} \cdot \frac{\left(\frac{Y}{S}\right)^s}{\alpha_1 + \alpha_2 \bar{\theta}^2} = \dot{\bar{\epsilon}} \cdot \frac{\left(\frac{Y}{S}\right)^s}{\alpha_1 + \alpha_2 \bar{\theta}^2} \quad \text{if } (\bar{\epsilon} > \epsilon_{D0} \cdot \exp\left(A \frac{-p}{\bar{\sigma}}\right) \text{ and } \frac{-p}{\bar{\sigma}} > \eta_c), \quad (2c)$$

$$\dot{D} = 0 \quad \text{otherwise}, \quad (2d)$$

where S and s are 2 material damage parameters, E and ν Young's modulus and Poisson's ratio, $\dot{\lambda}$ the plastic multiplier, $\bar{\epsilon}$ and $\dot{\bar{\epsilon}}$ the equivalent strain and strain rate. If $\alpha_2 = 0$ and $\alpha_1 = 1$, the standard Lemaitre model (Lemaitre and Desmorat (2005)) is resumed. The energy density release rate Y keeps its usual form. Eq(2c) states that damage variable D grows only after a certain threshold strain ϵ_{D0} , which is made here triaxiality-dependent, and if the state of stress is not too compressive (parameterized by η_c). Finally, the coupled character of the model is expressed by:

$$\sigma_{ij}^{eff} = \frac{\sigma_{ij}}{1-D}, \quad \bar{\sigma} = w(D) \cdot \sigma_{matrix}, \quad E = w(D) \cdot E_{matrix}, \quad (3a,b)$$

$$\text{if } \frac{-p}{\bar{\sigma}} \geq \eta_{c1} \quad w(D) = 1 - D, \quad (3c)$$

$$\text{if } \eta_{c1} > \frac{-p}{\bar{\sigma}} \geq \eta_{c2} \quad w(D) = 1 - \frac{(1-h) \cdot \frac{-p}{\bar{\sigma}} + h \eta_{c1} - \eta_{c2}}{\eta_{c1} - \eta_{c2}} \cdot D, \quad (3d)$$

$$\text{if } \frac{-p}{\bar{\sigma}} < \eta_{c2} \quad w(D) = 1 - h \cdot D, \quad (3e)$$

Eqs. (3b-e) mean that material weakening by damage is all the stronger as the state of stress is more tensile, the so-called crack closure effect in compression. This difference between compression and tension, characterized by h ($h = 0.2$ according to Lemaitre and Desmorat, 2005), is applied gradually between triaxialities η_{c1} and η_{c2} .

2.2. Fracture strain-based models

Bai and Wierzbicki (2008) propose to define the damage variable $D_{B\&W}$ by comparison of the current strain with a fracture strain $\bar{\varepsilon}_f$ which depends on triaxiality and Lode angle (D_i 's are 6 material parameters):

$$\bar{\varepsilon}_f\left(\frac{p}{\sigma}, \bar{\theta}\right) = \frac{1}{2}\bar{\theta}^2\left(D_1 \cdot \exp\left(D_2 \frac{p}{\sigma}\right) + D_5 \cdot \exp\left(D_6 \frac{p}{\sigma}\right) - 2D_3 \cdot \exp\left(D_4 \frac{p}{\sigma}\right)\right) + \frac{1}{2}\bar{\theta}\left(D_1 \cdot \exp\left(D_2 \frac{p}{\sigma}\right) - D_5 \cdot \exp\left(D_6 \frac{p}{\sigma}\right) + D_3 \cdot \exp\left(D_4 \frac{p}{\sigma}\right)\right), \quad (4)$$

$$D_{B\&W}(\bar{\varepsilon}) = \int_0^{\bar{\varepsilon}} \frac{d\bar{\varepsilon}}{\bar{\varepsilon}_f\left(\frac{p}{\sigma}, \bar{\theta}\right)}, \quad (5)$$

Xue (2007) also bases his analysis on a triaxiality- and Lode parameter-dependent fracture surface, but he builds a coupled model where the mechanical properties depend on damage:

$$\bar{\varepsilon}_f(p, \bar{\theta}) = \varepsilon_{f0} \cdot \left(\gamma + (1 - \gamma)|\bar{\theta}|^k\right) \cdot \left(1 - q \cdot \ln\left[1 - \frac{p}{p_L}\right]\right), \quad (6)$$

$$\dot{D}_{Xue} = m \left(\frac{\bar{\varepsilon}}{\bar{\varepsilon}_f(p, \bar{\theta})}\right)^{m-1} \frac{\dot{\bar{\varepsilon}}}{\bar{\varepsilon}_f(p, \bar{\theta})}, \quad (7a)$$

$$\bar{\sigma} = (1 - D_{Xue}^\beta) \cdot \sigma_{matrix}, \quad (7b)$$

γ is the ratio of damage under shear and under tension, p_L a critical pressure above which damage does not grow. Here, $k = 2$ and $\beta = 1$ are chosen.

2.3. Gurson-Tvergaard-Needleman and related models

The standard Gurson-Tvergaard-Needleman model is based on a pressure-dependent compressible plasticity:

$$\phi(p, \bar{\sigma}) = 0 = \left(\frac{\bar{\sigma}}{\sigma_0}\right)^2 + 2q_1 f^* \cosh\left(-\frac{3q_2}{2} \frac{p}{\sigma_0}\right) - (1 + (q_1 f^*)^2), \quad (8)$$

where σ_0 is the yield stress in tension of the matrix material. Porosity f , taken as the damage variable, grows according to the normal flow rule (the plastic strain rate tensor is named $\dot{\varepsilon}$, its plastic part is $\dot{\varepsilon}^{pl}$):

$$\dot{f}_{growth} = (1 - f) \cdot \text{trace}(\dot{\varepsilon}^{pl}), \quad (9)$$

The model also allows random cavity nucleation during the deformation process, so that:

$$\dot{f} = \dot{f}_{growth} + \dot{f}_{nucleation}, \quad (10a)$$

$$\dot{f}_{nucleation} = \frac{f_N}{s_N \cdot \sqrt{2\pi}} \cdot \exp\left(-\frac{1}{2} \left(\frac{\bar{\varepsilon} - \varepsilon_N}{s_N}\right)^2\right) \cdot \dot{\bar{\varepsilon}}, \quad \varepsilon_N = \varepsilon_{N0} \cdot \exp\left(B \cdot \frac{p}{\sigma}\right), \quad (10b,c)$$

The nucleation term is a Gaussian function of the plastic strain (Chu and Needleman (1980)) and the value of mean plastic strain at maximal nucleation depends on stress triaxiality ratio as proposed by (Cao et al. (2014b)).

Coalescence takes place beyond a critical porosity value f_c ; the real porosity is henceforward replaced by an “effective porosity” f^* :

$$\text{If } f < f_c \quad f^* = f, \quad \text{If } f > f_c \quad f^* = f_c + (f - f_c) \cdot \frac{f_u^* - f_c}{f_f - f_c}, \quad (11a,b)$$

The Gurson-Tvergaard-Needleman model is known to underestimate damage in the case of shear loading. Improvements have been proposed (Nahshon and Hutchinson (2008)), (Xue (2008)); the latter's modification is used here. It adds a "shear" damage term involving the Lode parameter:

$$\dot{D}_{shear} = q_3^* \cdot f^{q_4} \cdot (1 - |\bar{\theta}|) \cdot \bar{\epsilon} \cdot \dot{\bar{\epsilon}}, \quad \dot{D} = \Delta \cdot (q_1 \cdot \dot{f} + \dot{D}_{shear}), \quad (12,13)$$

Δ represents the effect of coalescence:

$$\text{If } D < q_1 \cdot f_c^* \quad \Delta = 1, \quad \text{If } 1 \geq D > q_1 \cdot f_c^* \quad \Delta = \frac{f_u^* - f_c^*}{f_f - f_c^*}, \quad (14a,b)$$

2.4. Finite Element Model and experimental identification of parameters

All models are implemented in Forge, an implicit, 3D Finite Element software based on (V,p) formulation using mini-elements (Mocellin et al. (2001)). Identification of the parameters of the models above, plus those describing work-hardening, has been performed using a set of experiments covering the $(\frac{-p}{\sigma}, \bar{\theta})$ plane: cylinder compression (-1/3;-1); torsion (0;0); plane-strain, flat grooved specimen (2/3-1;0); round and notched bar tension (1/3-2/3;1). The model has been used for this purpose (Cao (2013)). For Gurson-Tvergaard-Needleman - like models, X-Ray microtomography has been used also to identify nucleation parameters and porosity at fracture (Cao et al. (2014b)).

3. Wire-drawing + flat rolling forming sequence

3.1. Material and process description

Starting from a 14 mm diameter hot rolled and patented C62 high carbon perlitic steel wire, a flat section is formed in 4 wire-drawing and 3 flat rolling passes (see Massé (2010) for more details). As usual, wire drawing gives a generalized tension state on the centerline of the wire (positive triaxiality, $\bar{\theta} = 1$), where damage is most liable to occur. In the longitudinal cross section, the diagonals of the plastic zone are under generalized shear (near-zero triaxiality, $\bar{\theta} = 1$). In the rolling stage, strain rate clearly shows the "blacksmith's cross" heterogeneous deformation pattern in a transverse cross-section, which induces highly tensile episodes and makes this process at risk. The state of stress is unmistakably tensile on the edge: $(\frac{-p}{\sigma}, \bar{\theta}) = (0.3;1)$, because the metal is compressed and elongated only in the central part, whereas the edge has to follow this elongation without contact. The center and the arms of the cross are in a state intermediate between shear and compression.

3.2. Results

Fig. 1 and 2 show damage during wire-drawing and during wire flat rolling respectively. With the exception of the Gurson-Tvergaard-Needleman model completed by Xue, maximum damage is always in the center in wire-drawing, corresponding to a depressive state of stress (triaxiality above 0.2). The shear component grows from the center (zero shear due to the symmetry axis) to the surface (maximum curvature of the flow lines). As a consequence, Lode-enhanced models distribute damage more evenly along the radius. Compared with the other models, the Gurson-Tvergaard-Needleman + Xue model, Eqs. (12-14), overestimates the effect of shear; note however that the damage variable remains very small, $D < 0.002$, compared with its value at break, $D_c = 0.98$.

In rolling (Fig. 2), Lemaitre's model gives maximum damage on the edge, with a small secondary peak at the center corresponding to the heritage of wire-drawing. On the contrary, its shear-enhanced version ("LEL") depicts the blacksmith's cross. The same difference can be found between Gurson-Tvergaard-Needleman ("porosity") and shear-enhanced Gurson-Tvergaard-Needleman ("Dx-GTN"), although both locate the most damaged area in the center, similar to experiments (see (Massé (2010), or Cao (2013))). The Bai & Wierzbicki model ("B&W") is close to Gurson-Tvergaard-Needleman, whereas Xue's model resembles the enhanced Lemaitre model.

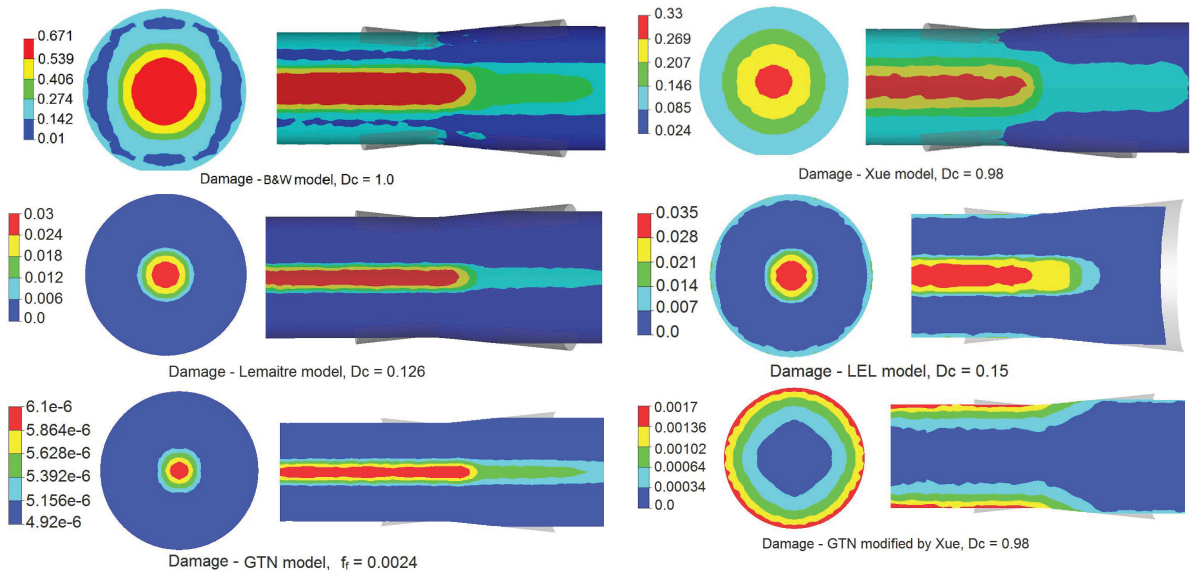


Fig. 1. Damage after 2 passes of wire-drawing. The values of damage at break (D_c, f_t) for each particular model is given under each figure.

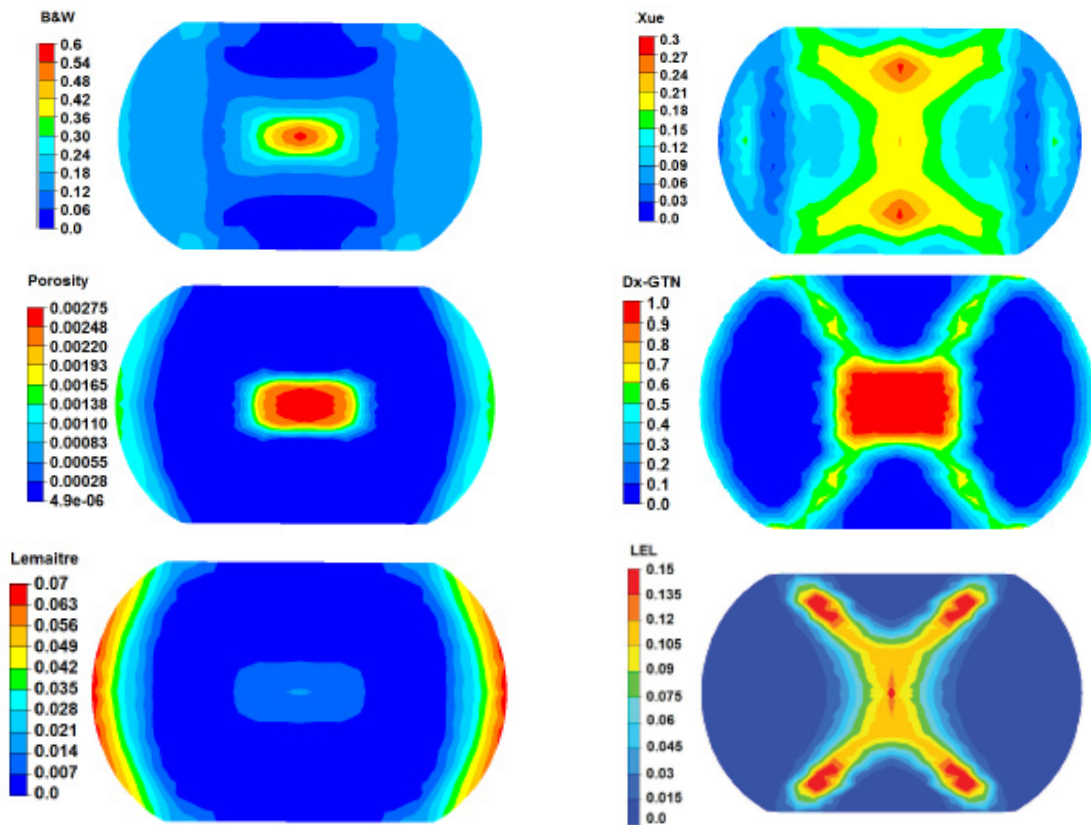


Fig. 2. Damage maps after 4 passes of wire-drawing and 1 pass of rolling.

Wire-drawing has been prolonged until wire broke at pass #14. The simulation indicates when D_c (or f_f) is reached at the most damaged location in the material. Comparison with the experimental number of passes at break is a strong test of the models. For the Bai and Wierzbicki model, damage grows linearly and reaches fracture at the 4th pass. Coupled models such as Lemaitre or Xue also predict fracture much too early. The behavior of the Gurson-Tvergaard-Needleman model is more interesting. Starting from an initial $f_0 \approx 10^{-6}$, porosity remains very small (although slowly growing) during the first 4 passes. Then a jump is found during passes 5 and 6, the strain range in which nucleation takes place ($\varepsilon_N \pm 3S_N$, Eq. (10b)). Later on, as no cavity can nucleate any more, a slow growth regime is resumed, due to the moderately depressive nature of the process, until the critical fracture porosity $f_f = 0.0024$ (identified by microtomography) is reached at pass #13 – by far the best fit.

4. Conclusion

Six damage models from the recent literature have been implemented, their parameters identified from experiments, and their performance tested on different cold forming schedules. Note that the sets of parameters identified by laboratory mechanical tests have been used “as is”, without any modification, to study wire-drawing and wire rolling. The experimental trends in terms of time and location of failure have been checked. In the wire-drawing of patented high carbon steel, the Gurson-Tvergaard-Needleman model is the one which best fits measurements. Other models (Lemaitre, Bai & Wierzbicki) predict a largely premature failure.

Coming to rolling, experimental void density maps can be reproduced only with shear-emphasizing damage models. It is quite difficult to obtain a good balance between the lateral surfaces (low but non negligible porosity), the center (largest density) and the arms of the blacksmith’s cross (intermediate). Again, Gurson-Tvergaard-Needleman is globally the best if used with shear-enhancement (here, the Xue phenomenological formulation).

Acknowledgements

The authors gratefully thank ArcelorMittal, Ugitech and AREVA for funding and for permission to publish.

References

- Lemaitre, J., 1986. Local approach of fracture. *Engineering Fracture Mechanics* 25 (5-6), 523-537.
- Bai, Y., Wierzbicki, T., 2008. A new model of metal plasticity and fracture with pressure and Lode dependence. *International Journal of Plasticity* 24 (6), 1071-1096.
- Xue, L., 2007. Damage accumulation and fracture initiation in uncracked ductile solids subject to triaxial loading. *International Journal of Solids and Structures* 44 (16), 5163-5181.
- Needleman, A., Tvergaard, V., 1984. An analysis of ductile rupture in notched bars. *Journal of the Mechanics and Physics of Solids* 32 (6), 461-490.
- Nahshon, K., Hutchinson, J., 2008. Modification of the Gurson Model for shear failure, *European Journal of Mechanics – A/Solids* 27 (1) 1–17.
- Xue, L., 2008. Constitutive modeling of void shearing effect in ductile fracture of porous materials. *Engineering Fracture Mechanics* 75 (11), 3343-3366.
- Massé, T., Chastel, Y., Montmitonnet, P., Bobadilla, C., Persem, N., Foissey, S., 2012. Mechanical and damage analysis along a at-rolled wire cold forming schedule. *International Journal of Material Forming* 5 (2), 129-146.
- Cao, T.-S., Gachet, J.-M., Montmitonnet, P., Bouchard, P.-O., 2014a. A Lode-dependent enhanced Lemaitre model for ductile fracture prediction at low stress triaxiality. In the press, *Engineering Fracture Mechanics*.
- Lemaitre, J., Desmorat, R., 2005. *Engineering Damage Mechanics: Ductile, Creep, Fatigue and Brittle Failures*. Springer, Berlin.
- Chu, C.C., Needleman, A., 1980. Void nucleation effects in biaxially stretched sheets. *Journal of Engineering Materials and Technology*, 102(3): 249-256.
- Cao, T.-S., Maire, E., Verdu, C., Bobadilla, C., Lasne, P., Montmitonnet, P., Bouchard P.-O., 2014b. Characterization of ductile damage for a high carbon steel using 3D X-ray micro-tomography and mechanical tests - Application to the identification of a shear modified GTN model, *Computational Materials Science*, 84:175-187.
- K. Mocellin, L. Fourment, T. Coupez and J.-L. Chenot, 2001. Toward large scale FE computation of hot forging process using iterative solvers, parallel computation and multigrid algorithms. *International Journal for Numerical Methods in Engineering* 52, 473-488.
- Massé, T., 2010. Study and optimization of high carbon steel at wires. PhD Dissertation, Ecole Nationale Supérieure des Mines de Paris.
- Cao, T.-S., 2013. Modeling ductile damage for complex loading paths. PhD Dissertation, Ecole Nationale Supérieure des Mines de Paris.